Magnetic field evolution and reconnection in low resistivity plasmas

Allen H Boozer
Columbia University, New York, NY 10027
ahb17@columbia.edu
(Dated: December 16, 2022)

A driven evolution of a magnetic field has three aspects: field line topology, magnetic energy, and magnetic helicity. An ideal evolution with minimal energy input can produce magnetic field line chaos, which makes the preservation of field-line topology exponentially sensitive to non-ideal effects on an evolution timescale, but has no direct effect on energy or helicity dissipation. Resistive dissipation of the power input requires highly localized current densities $j \approx vB/\eta$, where v is the velocity given by the evolution drive and η is the plasma resistivity. Dissipation of the magnetic helicity input cannot be balanced when the magnetic Reynolds number is large compared to unity. Current densities $j \approx vB/\eta$ are consistent with those required to produce the solar corona with the observed height of the transition region by the Dreicer electron runaway effect.

I. INTRODUCTION

According to Wikipedia: *Magnetic reconnection is a physical process occurring in highly conducting plasmas in which the magnetic topology is rearranged and magnetic energy is converted to kinetic energy, thermal energy, and particle acceleration.*

Magnetic topology rearrangement and magnetic energy conversion are two distinct physical processes, but each process has been used to define magnetic reconnection. The classical definition was in a 1956 paper of Parker and Krook [1]: *severing and reconnection of lines of force.* In the space sciences, the emphasis has focused on energy conversion. In 2020, Hesse and Cassak stated [2]: *Magnetic reconnection converts, often explosively, stored magnetic energy to particle energy in space and in the laboratory.*

By definition, a highly conducting plasma has a magnetic Reynolds number,

$$R_m \equiv \frac{\mu_0 v a}{\eta}, \tag{1}$$

that is far larger than unity; v is a typical plasma flow speed, a a typical spatial scale, and η/μ_0 is the resistive diffusion coefficient. In problems of interest R_m can be between 10^4 and 10^{14}.

A practical understanding of magnetic field evolution when the magnetic Reynolds number, R_m, is large requires disentangling three distinct physical processes: magnetic topology rearrangement, magnetic energy conversion , and magnetic helicity evolution. This disentanglement depends on whether the magnetic field depends non-trivially on all three spatial coordinates or only two.

The classic paradigm for magnetic reconnection was that of Schindler, Hesse, and Birn [3]. They noted that

$$\frac{\partial \vec{B}}{\partial t} = \vec{\nabla} \times \left(\vec{v} \times \vec{B} + \eta \vec{j} \right) \tag{2}$$

implies that resistive breaking of the magnetic field lines directly competes with an evolution velocity $\vec{v}$ when the current density lies in a narrow sheet of cross-sectional area a^2/R_m with a magnitude that approximates

$$j_{shb} \equiv \frac{vB}{\eta}. \tag{3}$$

The classic reconnection paradigm of Schindler et al was developed for reconnection in which the magnetic field has a non-trivial dependence on only two spatial coordinates. A different paradigm for the breaking of magnetic field line connections has been introduced when the magnetic field has a non-trivial dependence on all three spatial coordinates. The three dimensional case is the one of practical interest, but most of the literature is focused on the two dimensions, which excludes magnetic field line chaos.

By definition, magnetic field lines are chaotic when neighboring pairs of lines separate exponentially with distance along the lines while remaining within a bounded region of space. A basic result is that magnetic field lines can go from a simple smooth form to having large and broadly-spread changes in their connections on a timescale that is approximately a factor of ten longer than the ideal evolution time when and only when the magnetic field lines become chaotic.

The centrality of chaos to the rapid onset of changes in magnetic topology when the plasma resistivity and other non-ideal effects are small is controversial and could be shown to be false in two ways: (1) Find an evolving highly chaotic magnetic field that nonetheless preserves well-defined magnetic field line connections. (2) Find an evolving non-chaotic magnetic field that nonetheless goes from being simple and smooth to large scale connection breaking on a timescale only an order of magnitude longer than the ideal evolution time, even when R_m is many orders of magnitude larger than unity.

The statement about the importance of chaos can never be proven to be correct. Karl Popper, one the twentieth century's most influential philosophers of science, famously stated [4] that a scientific statement can never be proven to be correct but that it must in principle be testable. The most reliable scientific statements have been tested and never proven false. Popper's statements should be kept in mind while considering the importance of chaos to reconnection.

Huang and Bhattacharjee [5] recently published a paper *Do chaotic field lines cause fast reconnection in coronal loops?* When the evolution forces the field lines to become chaotic, they found the onset of changes in field-line connections occurs on a timescale set by the evolution essentially independent of the resistivity. Nevertheless, they implied the answer to their question was negative because the energy transfer, which occurs on a timescale approximately a factor of two longer, requires a much higher current density than that required for sufficiently strong chaos for the breaking of magnetic field line connections. Section VI discusses their paper, which is skeptical about relevance of chaos while confirming the central tenets of its role in reconnection. Most of the reconnection literature ignores chaos rather than testing its importance.

The importance of chaos to the breaking of magnetic field line connections is intuitively obvious. When an evolving magnetic field has a non-trivial dependence on all three spatial coordinates, a tube of contiguous magnetic field lines generally undergoes an exponential distortion with distance along the tube with the distortion increasing as the evolution progresses. This distortion is illustrated for the model of Figure 1 a in Figure 1 b from the paper by Huang and Bhattacharjee. Different tubes become exponentially close at some points and are distant at others. As the distortion increases, even the smallest non-ideal effects such as resistivity will intermix field lines from different tubes. The importance of this effect to producing fast changes has been developed in a number of papers by Boozer, recent papers include [6] and by Boozer and Elder [7]. The current density required to obtain reconnection due to chaos is $j \approx (B/\mu_0 L) \ln R_m$ and the required timescale is approximately $(a/v) \ln R_m$. This current density lies in multiple thin but broad ribbons along the magnetic field lines.

Magnetic field line chaos implies that the current density j_{shb} defined by Schindler, Hesse, and Birn is not required for a rapid change in magnetic field line connections; only $j \approx (B/\mu_0 L) \ln R_m$ is needed for that. However, a current density comparable to j_{shb} is required for Ohmic dissipation to balance the power input when the magnetic evolution is maintained by driving a velocity v, as is the model of Figure 1 a.

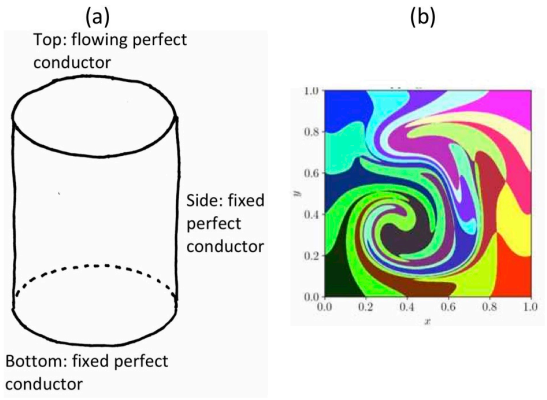

FIG. 1: (a) A perfectly conducting cylinder of height L and radius a encloses an ideal pressureless plasma. All of the sides of the cylinder are fixed except the top, which flows with a specified velocity $\vec{v}_t$. Initially, $\vec{B} = B_0\hat{z}$. Each point $\vec{x}_b$ on the bottom of the cylinder defines a line of $\vec{B}$ that in an ideal evolution intercepts a specific point on the top $\vec{x}_t$ with $\partial\vec{x}_t(\vec{x}_0,t)/\partial t = \vec{v}_t(\vec{x}_t,t)$ and $\vec{x}_0 \equiv \vec{x}_t$ at $t = 0$. The case of primary interest is when $\vec{v}_t$ is divergence free and chaotic. This means the 2×2 Jacobian matrix $\partial\vec{x}_t/\partial\vec{x}_0$ has a large singular value that increases exponentially in time and a small singular value that is the inverse of the large singular value. This figure was originally published in Reference [7]. (b) Huang and Bhattacharjee [5] used an equivalent square-cylindrical model to project images on the top boundary of square tubes of magnetic field lines on the bottom boundary. As the distortions become ever larger, an arbitrarily small resistive diffusion η/μ_0 can intermix field lines from different tubes and thereby change their connections. This figure is part of Figure 5 of their paper.

As discussed in Section V, when the drive for the magnetic evolution is the flow in a sunspot that is a footpoint for a coronal loop, j_{shb} equals the current required for electron runaway at the approximate height of the transition region to the solar corona. In other words, the observed solar corona can be taken as evidence that current densities $j \sim j_{shb}$ actually arise in the photosphere. The timescale required for the current density to become this large is discussed in Sections III and VI A 3.

Papers by a number of authors emphasize that chaotic magnetic-field-line trajectories fundamentally change the paradigm of magnetic reconnection from that of Schindler et al. In 2005, Borgogno, Grasso, Porcelli, Califano, Pegoraro, and Farina showed that the interaction of tearing modes with different helicities in toroidal plasmas creates magnetic field chaos and fundamentally changes the definition of magnetic reconnection from the case in

which the magnetic field depends on only two spatial coordinates [8]. Chaos enters the theory of turbulent magnetic reconnection, and this topic was reviewed [9] by Lazarian, Eyink, Jafari, Kowal, Li, Xu, and Vishniac in 2020. Eric Priest is associated with a large body of work on three-dimensional structures that tend to concentrate currents and thereby lead to enhanced reconnection [10]. In particular, he is known for his work on quasi-separatrix layers, which are essentially regions of field line chaos. Reid, Parnell, Hood, and Browning [11], have simulated a case in which the footpoint motions of magnetic field lines do not directly make the lines chaotic but drive large-scale instabilities that do. Huang and Bhattacharjee [5] recognize that magnetic fields that depend on all three spatial coordinates are generically chaotic and that the chaos makes the maintenance of field line connections fragile. Their simulations agree with those of Boozer and Elder [7] in the build up towards point at which a change in field-line connections becomes inevitable. This is the only period Boozer and Elder simulated.

The two defining processes for reconnection, a topology change in the magnetic field lines or an energy change in the magnetic field, are only weakly coupled. Tokamak disruptions are spectacular changes in field-line topology. Most of the magnetic surfaces can be destroyed and the current profile flattened on a timescale of milliseconds, when the naively expected timescale would be minutes. But, the change in the poloidal field energy [12] is $\sim$7.5% with the poloidal field energy only a few percent of the magnetic field energy in the plasma. It is the constraint of magnetic-helicity conservation that limits the release of energy. On the other hand, ideal instabilities can convert magnetic energy into plasma motion on an Alfvénic time scale with no changes in the connections of the magnetic field lines. Nevertheless, the non-linear evolution of ideal instabilities may result in rapid changes in magnetic field line connections no matter how small the resistivity may be [11, 13, 14].

Magnetic field line chaos exponentially shortens the time required before field lines can undergo topological changes but has little direct effect on the rate of energy dissipation and no effect on the rate of helicity change. The robustness of magnetic helicity conservation has been known since the 1984 work of Berger [15]. The essential point is that the resistive change in the helicity is given by $\int \eta \vec{j} \cdot \vec{B} d^3x$, but resistive dissipation of energy is given by $\int \eta j^2 d^3x$. Concentrating the current in a thin channel enhances the energy dissipation but not the rate of helicity change. As discussed by Boozer and Elder when the timescale for helicity injection is shorter than the resistive timescale defined by the spatially averaged parallel current, flux-tube eruption must eventually occur [7].

The role of helicity conservation in the space sciences is most prominent in the theory of dynamos, which is closely related to the theory of reconnection. The conservation properties of the helicity have been known since 1986 to invalidate the α-effect dynamo [16]. A more detailed proof was given in 1995 by Bhattacharjee and Yuan [17]. Nevertheless, the α-effect dynamo is commonly studied in dynamo simulations [18] by having a model that destroys helicity at small scales even though this is not energetically possible.

Although simulations are important for studying the physics of reconnection, simulations are limited to small magnetic Reynolds numbers $R_m \lesssim 10^6$ due to the higher resolution required as R_m increases. The resolution in each of the three spatial spatial directions as well as time must be increased as R_m. The implications of chaos at $R_m = 10^{14}$ requires analytic understanding.

This paper has seven sections: Section II, *Differences in paradigms*, discusses the different views on what are the important reconnection features and questions. These differences are most apparent between studies of toroidal magnetic-fusion plasmas and studies of space and astrophysical plasmas.

Section III, *Rate of current density increase*, explains two ways to analytically study the rate at which the current density increases: the increase in the parallel current along an arbitrarily chosen magnetic field line and the increase in the current density in a given flow.

Section IV, *Evolution equations for magnetic field connections, energy, and helicity*, derives the three basic evolution equations and discusses their consequences.

Section V, *Runaway electrons and the corona*, explains why the existence of the solar corona provides evidence that a parallel current density comparable to j_{shb} is driven from sunspots on the photosphere.

Section VI *Simulations by Huang and Bhattacharjee*, discusses the primary simulation [5] of the effect of a chaotic drive for magnetic field evolution.

Section VII summarizes the paper.

II. DIFFERENCES IN PARADIGMS

In 1962, Thomas Kuhn [19] in *one of the most influential works of history and philosophy written in the 20th century* [20], discussed how differences in the important questions and in the important features of a model arise whenever a new paradigm is introduced. He also pointed out how difficult it is for a scientific community to accept a change in

paradigm.

Different views about what are the important questions in reconnection theory and what are the important features of a model are most apparent between studies of toroidal magnetic-fusion plasmas and studies of space and astrophysical plasmas.

A. Differences in questions

The questions that are considered important are different between studies of magnetic-fusion and space plasmas. (1) When the initial condition of an evolving magnetic field is smooth, is the time required for reconnection to occur on a timescale comparable to the timescale set by an evolution? This is a central issue in tokamak disruptions but the onset time for reconnection has not been a focus in space and astrophysical plasmas. (2) How should the speed of reconnection be defined? When rapid energy transfer from the magnetic field to the plasmas is the definition of reconnection then the rate of transfer provides a definition.

When a rapid breaking of the toroidal magnetic surfaces occurs in a tokamak, the definition of the speed of reconnection is subtle. Magnetic field lines are defined at points in time. When the last intact magnetic surface is broken, a magnetic field line at that instant changes from being bound by that surface to traversing the plasma and striking the chamber walls. The relevant speed is not defined by the instantaneous change in the trajectory of the field line but by the speed of physical effects that are produced by the topological change. For example, the topological change can allow relativistic electrons trapped in the core of a tokamak to strike the surrounding walls by following magnetic field lines. The damage to the device is largely determined by how highly localized in space and time are the strikes of the relativistic electrons on the walls.

In space and astrophysical studies, little study is done of the physical effects produced by the changes in field line connections. Studies are focused on energy transfer from the fields to the plasma and on acceleration of particles by the reconnection process. Although the acceleration of electrons to relativistic energies as a result of magnetic surface reconnection is a major issue in tokamaks, the acceleration is not a direct part of the reconnection process but rather a result of the plasma cooling increasing the resistivity to the point that $\eta\bar{j}$, with $\bar{j}$ a spatially-averaged current density, gives an electric field above that required for electron runaway.

B. Differences in problems

The periodicity of toroidal fusion plasmas gives a clear definition of the breaking of magnetic connections. Breaking connections means breaking magnetic surfaces, as in a tokamak disruption. In space plasmas the boundary conditions are often too indeterminate to rigorously define magnetic field line topology or what is meant by the breaking of field-line connections. Nevertheless, answers to physical questions within the region of interest may depend on what happens outside that region [21].

When the breaking of field-line connections is not defined, the effects and speed of braking connections are treated as unimportant.

In toroidal fusion plasmas, the effects of magnetic surface breaking are of primary importance—the loss of plasma confinement and the flattening of $j_{||}/B$ over each regions covered by a single field line. Changes in field line topology occurs at instants in time. Nevertheless, the effects of topological changes occur over finite time intervals, the time it takes for particles or energy to be transported along magnetic field lines throughout a chaotic region. For $j_{||}/B$ flattening, the characteristic time is the time for shear Alfvén waves to cover the chaotic region by propagating along the magnetic field lines.

When topology and changes in field line connections are ill-defined, energy transfers between the field and the plasma seem most important, and it is natural to define magnetic reconnection by the energy transfer [2]. Energy transfer can be defined even in models in which changes in magnetic topology are not defined. A non-zero η is unnecessary for energy release from the magnetic field–ideal magnetic kinks are a well known example. Nevertheless, the energy release from the magnetic field is generally greater when the field-line connections are freely broken. The direct energy release from the magnetic field is of little interest in the fast reconnections called tokamak disruptions for as mentioned earlier less than a part in a thousand of the energy is typically released [12].

III. RATE OF CURRENT DENSITY INCREASE

The increase in the current density along an arbitrarily chosen magnetic field line and the increase in the current density in a given flow are the two ways to estimate the rate the plasma current increases.

A. Current density along an arbitrary line of $\vec{B}$

1. The near-line expansion

When the ideal evolution term, $\vec{v}\times\vec{B}$, is large compared to the resistive term, the evolution of the parallel current $j_{||}$ along an arbitrarily chosen magnetic field line $\vec{x}_0(\ell,t)$ is given by [22, 23]

$$\frac{\partial\Omega B_0}{\partial\ell} = \frac{\partial\left(K_0 + 2\tau_0 + \frac{4k_q^2}{\partial\varphi_q/\partial s}\right)B_0}{\partial t}. \tag{4}$$

$K(\ell,t)\equiv\mu_0 j_{||}/B_0$, $\Omega(\ell,t)=\hat{b}_0\cdot\vec{\nabla}\times\vec{v}$, and $\tau_0(\ell,t)$ is the torsion of the curve. The quantity $k_q^2/(\partial\varphi_q/\partial\ell)$ is defined by the quadrupole contribution to the Hamiltonian for the adjacent magnetic field lines and should only be retained when the adjacent field lines are not chaotic.

A more intuitive and more easily interpreted form of Equation (4) is

$$\frac{\partial\Omega B_0}{\partial\ell} = \frac{\partial\left(K_0+2\nu\right)B_0}{\partial t}, \tag{5}$$

where $\nu(\ell,t)$ is the stellarator-like rotational transform per unit length of field lines produced by currents at a distance from the chosen line. The term on the right-hand side of Equation (5) comes from the fact that when the externally-produced rotational transform ν per unit length has a positive time derivative, then K must decrease to keep the total transform per unit length fixed. The factor of two comes from dependence of the current-produced transform at a radius ρ_0 being proportional to $(\int K\rho d\rho)/\rho_0^2 = K/2$ as $\rho_0\to 0$. The left-hand side comes from the fact that when the field lines are undergoing a twist per unit time, which is what Ω is, then a current must increase to produce a total rotational transform per unit length that gives $\partial\Omega/\partial\ell$.

The derivation of Equation (4) uses the position vector is $\vec{x}(\rho,\alpha,\ell)=\rho\cos\alpha\hat{\kappa}_0+\rho\sin\alpha\hat{\tau}_0+\vec{x}_0(\ell,t)$, where ρ is the distance from the curve; $\hat{\kappa_0}$ and $\hat{\tau}_0$ are the curvature and torsion unit vectors of the field line $\vec{x}_0(\ell,t)$. The trajectories of the adjacent lines are given by a $\tilde{H}=\tilde{\psi}h(\alpha,s)$, where $h=k_\omega(s,t)+k_q(s,t)\cos\left(2\alpha-\varphi_q(s,t)\right)$ with $k_\omega\equiv K_0/2+\tau_0$. The magnitude of the quadrupole component of the magnetic field is given by $k_q\tilde{\psi}$, the only ρ^2 order Fourier component in the Hamiltonian. The magnetic flux is $\tilde{\psi}\equiv\pi B_0\rho^2$.

2. Analogous expression of Huang and Bhattacharjee

Equation (15) of Huang and Bhattacharjee [5] appears to be analogous to Equation (5). Their analogue to $2\partial\nu(\ell,t)/\partial t$ is $\mathcal{T}$, where

$$\mathcal{T}\equiv\partial_x\vec{u}\cdot\partial_y\vec{B}_\perp - \partial_y\vec{u}\cdot\partial_x\vec{B}_\perp. \tag{6}$$

Their paper emphasizes the importance of $\mathcal{T}$ to the differences between their results and those of Boozer and Elder [7].

Near a given line the divergence-free magnetic field line velocity and the ideal perturbation to the magnetic field $\delta\vec{B}$ can be written in terms of the field line displacement $\vec{\Delta}$ with $\vec{\nabla}\cdot\vec{\Delta}=0$;

$$\begin{aligned}
\vec{u} &= \frac{\partial\vec{\Delta}}{\partial t}; && (7)\\
\delta\vec{B} &= \vec{\nabla}\times(\vec{\Delta}\times B_0\hat{z}) && (8)\\
&= B_0\frac{\partial\vec{\Delta}}{\partial z}. && (9)
\end{aligned}$$

The displacement is the sum of two parts: a part with a curl, $\vec{\Delta}_c$, and a quadrupole part, Δ_q, that does not. Each has an associated velocity and perturbed magnetic field. The displacement Δ_c also has an associated vorticity Ω and a parallel current density, or K, but Δ_q does not.

$$\begin{aligned}
\vec{\Delta}_c &= \Delta_{c1}(z,t)x\hat{y} - \Delta_{c2}(z,t)y\hat{x}; && (10)\\
\Omega &\equiv \hat{z}\cdot\vec{\nabla}\times\vec{u}_c && (11)\\
&= \frac{\partial(\Delta_{c1}+\Delta_{c2})}{\partial t}; && (12)\\
\frac{\delta\vec{B}_c}{B_0} &= \frac{\partial\Delta_{c1}}{\partial z}x\hat{y} - \frac{\partial\Delta_{c2}}{\partial z}y\hat{x}; && (13)\\
K &\equiv \frac{\hat{z}\cdot\vec{\nabla}\times\delta\vec{B}_c}{B_0} && (14)\\
&= \frac{\partial(\Delta_{c1}+\Delta_{c2})}{\partial z}; && (15)\\
\vec{\Delta}_q &= \Delta_q(t)(x\hat{x}-y\hat{y})\cos(k_z z)\\
&\quad +\Delta_q(t)(y\hat{x}+x\hat{y})\sin(k_z z); && (16)\\
\delta\vec{B}_q &= k_z B_0\Big\{(y\hat{x}+x\hat{y})\cos(k_z z)\\
&\quad -(x\hat{x}-y\hat{y})\sin(k_z z)\Big\}. && (17)
\end{aligned}$$

The magnetic scalar potential that gives the dipolar field is proportional to $\rho^2\cos(2\theta-k_z z)$, where ρ is the distance from the line, and θ is the angle around the line. Only one Fourier component in z is retained, but an arbitrary number of k_z's could be. The second harmonic is the only curl-free term that can contribute in ρ^2 order.

The there are four contributions to $\mathcal{T}$ of Equation (6). $\mathcal{T}=\mathcal{T}_{cc}+\mathcal{T}_{cq}+\mathcal{T}_{qc}+\mathcal{T}_{qq}$ with first suffix denoting $\vec{u}_c$ or $\vec{u}_q$ and the second the corresponding $\delta\vec{B}$.

$$\mathcal{T}_{cc} = 0; \tag{18}$$

$$\mathcal{T}_{cq} = k_z B_0 \frac{\partial(\Delta_{c1}-\Delta_{c2})}{\partial t}\Delta_q \sin(k_z z); \quad (19)$$

$$\mathcal{T}_{cq} = B_0 \frac{\partial \Delta_q}{\partial t}\frac{\partial(\Delta_{c1}-\Delta_{c2})}{\partial z}\cos(k_z z); \quad (20)$$

$$\mathcal{T}_{qq} = k_z B_0 \frac{d\Delta_q^2}{dt}. \quad (21)$$

Letting $\Delta_{c1}-\Delta_{c2} = \Delta_c(t)\cos(k_z z) + \Delta_s(t)\sin(k_z z)$ gives

$$\begin{aligned}\mathcal{T} &= k_z B_0 \left(\frac{\Delta_q^2 + \Delta_s\Delta_q/2}{dt}\right) \\ &+k_z B_0\Big\{\left(\frac{d\Delta_c}{dt}\Delta_q - \Delta_c\frac{d\Delta_q}{dt}\right)\frac{\sin(2k_z z)}{2} \\ &+\left(\Delta_s\frac{d\Delta_q}{dt} - \frac{d\Delta_s}{dt}\Delta_q\right)\frac{\cos(2k_z z)}{2}\Big\}. \quad (22)\end{aligned}$$

When the various Δ's increase together, so $d\ln\Delta_c/dt = d\ln\Delta_s/dt = d\ln\Delta_q/dt$,

$$\mathcal{T} = k_z B_0 \left(\frac{\Delta_q^2 + \Delta_s\Delta_q/2}{dt}\right) \quad \text{and} \quad (23)$$

$$\nu_{hb} = k_z \frac{\Delta_q^2 + \Delta_s\Delta_q/2}{2a^2} \quad (24)$$

is the Huang and Bhattacharjee analogue of ν in Equation (5) using the coefficients that they used to make their equations dimensionless.

3. *Force-balance and plasma flow*

Once magnetic field lines have become chaotic, so connections are easily broken, the power input goes into plasma motion until it can be dissipated by resistivity or viscosity.

The divergence-free nature of the current $\vec{j}$ implies K and the Lorentz force $\vec{f}_L \equiv \vec{j}\times\vec{B}$ are related by

$$\frac{\partial K}{\partial \ell} = \hat{b}\cdot\vec{\nabla}\times\frac{\mu_0\vec{f}_L}{B^2}, \text{ where} \quad (25)$$

$$\vec{f}_L = \rho\left(\frac{\partial\vec{v}}{\partial t} + \vec{v}\cdot\vec{\nabla}\vec{v} - \nu\vec{\nabla}\times\vec{\Omega}\right). \quad (26)$$

When the linear inertial term dominates $V_A^2\partial K/\partial\ell = \partial\Omega/\partial t$ and K relaxes to being uniform along magnetic field lines at the Alfvén speed, V_A.

As discussed in Section VI, the behavior of $\partial K/\partial t$ depends on the relative magnitudes of $\partial\vec{v}/\partial t$, $\vec{v}\cdot\vec{\nabla}\vec{v}$, and $\nu\vec{\nabla}\times\vec{\Omega}$, which could be explored by simulations.

B. Current increase in a given flow

When the magnetic field lines have a known velocity, $\vec{u}_\perp(\vec{x},t)$, the Cauchy solution for the ideal evolution of the magnetic field is

$$\vec{B}\big(\vec{x}(\vec{x}_0,t)\big) = \frac{\overleftrightarrow{J}_L}{\mathcal{J}_L}\cdot\vec{B}(\vec{x}_0), \quad (27)$$

where $\overleftrightarrow{J}_L$ is the Jacobian matrix of the Lagrangian coordinates of $\vec{u}_\perp$ and $\mathcal{J}_L$ is the determinant of $\overleftrightarrow{J}_L$. The history of this solution was reviewed by Stern [24] in 1966.

Equation (27) has profound implications about the differences in between two and three dimensional evolution and the speed with which the current density can increase.

The Cauchy solution is a purely mathematical statement about Faraday's law, $\partial\vec{B}/\partial t = -\vec{\nabla}\times\vec{E}$, and the representation of the vector $\vec{E}$ in terms of $\vec{B}$. Widespread confusion exists within the reconnection community between this mathematical representation of $\vec{E}$ and Ohm's law, which is the constitutive expression for the electric field. This distinction is explained in Section III B 1.

Section III B 2 defines Lagrangian coordinates, $\vec{x}(\vec{x}_0,t)$, and explains the Singular Value Decomposition of the Jacobian matrix $\overleftrightarrow{J}_L \equiv \partial\vec{x}/\partial\vec{x}_0$. The implications of the Cauchy solution are discussed in Section III B 3.

1. *Electric field expression versus representation*

Two concepts that are commonly confused are the general representation of an electric field

$$\vec{E} + \vec{u}\times\vec{B} = -\vec{\nabla}\Phi + \mathcal{E}\vec{\nabla}\ell, \quad (28)$$

where $\mathcal{E}$ is constant along a magnetic field line [25], and an Ohm's law expression for the electric field, such as

$$\vec{E} + \vec{v}\times\vec{B} = \eta\vec{j} - \frac{\vec{\nabla}p_e}{en}, \quad (29)$$

where the term involving the gradient of the electron pressure divided by its density is called the Hall term.

Equation (28) is a purely mathematical statement about representation of one three-space vector, $\vec{E}(\vec{x},t)$, in terms of another, $\vec{B}(\vec{x},t)$. Its physical importance is that it clarifies the properties of evolving magnetic fields since that evolution is given exactly by Faraday's law, $\partial\vec{B}/\partial t = -\vec{\nabla}\times\vec{E}$. In particular, the magnetic evolution is called ideal when $\mathcal{E} = 0$;

then $\vec{u}_\perp$ is the velocity of the magnetic field lines, as shown by Newcomb [26] in 1958. The component of $\vec{u}$ along the field lines is arbitrarily defined, only the perpendicular components $\vec{u}_\perp$ are physically meaningful. Magnetic field lines that are evolving ideally become chaotic when the streamlines of $\vec{u}_\perp$ are chaotic. The topology of the magnetic field lines cannot change unless $\mathcal{E}$ is non-zero but becomes exponentially sensitive to a non-zero $\mathcal{E}$ when the streamlines of $\vec{u}_\perp$ are chaotic.

Although the validity of Equation (28) appears to depend on $\vec{B} \neq 0$, it is also valid in the presence of point nulls of $\vec{B}$. This is seen by placing an infinitesimal sphere around each point null as was done by Elder and Boozer [27] in 2021. The potential Φ at the null must be chosen to ensure $\oint \vec{j} \cdot d\vec{a} = 0$ at each null—charge cannot accumulate at a null. It should be noted that only point nulls are generic. Line nulls can be broken into well separated point nulls by a magnetic perturbation of infinitesimal strength.

On the other hand, Equation (29) of Ohm's law is a statement of physics, a constitutive relation, that gives one physical quantity, $\vec{E}(\vec{x}, t)$, in terms of others such as the mass flow velocity $\vec{v}(\vec{x}, t)$, and current density $\vec{j}(\vec{x}, t)$, of a plasma. The vector components of the right-hand side of Ohm's law that are perpendicular to $\vec{B}$ give the velocity $\vec{v}$ of the plasma relative to the velocity $\vec{u}$, which when, but only when, the magnetic evolution is ideal is the velocity of the magnetic field lines. When the Hall term is ignored and $|\vec{j}_\perp| << |j_{||}$, the velocity $\vec{u}$ can be identified with $\vec{v}$. To simplify discussions, $\vec{u}$ and $\vec{v}$ are frequently identified.

2. *Lagrangian coordinates*

Lagrangian coordinates $\vec{x}_0$ are defined so that the position vector in ordinary Cartesian coordinates is $\vec{x}(\vec{x}_0, t)$, where

$$\left(\frac{\partial \vec{x}}{\partial t}\right)_L \equiv \vec{u}_\perp(\vec{x}, t) \text{ with } \vec{x}(\vec{x}_0, t = 0) = \vec{x}_0. \quad (30)$$

The subscript "L" implies the Lagrangian coordinates $\vec{x}_0$ are held fixed.

The three-by-three Jacobian matrix of Lagrangian coordinates can be decomposed as

$$\frac{\partial \vec{x}}{\partial \vec{x}_0} \equiv \begin{pmatrix} \frac{\partial x}{\partial x_0} & \frac{\partial x}{\partial y_0} & \frac{\partial x}{\partial z_0} \\ \frac{\partial y}{\partial x_0} & \frac{\partial y}{\partial y_0} & \frac{\partial y}{\partial z_0} \\ \frac{\partial z}{\partial x_0} & \frac{\partial z}{\partial y_0} & \frac{\partial z}{\partial z_0} \end{pmatrix} = \overleftrightarrow{U} \cdot \begin{pmatrix} \Lambda_u & 0 & 0 \\ 0 & \Lambda_m & 0 \\ 0 & 0 & \Lambda_s \end{pmatrix} \cdot \overleftrightarrow{V}^\dagger. \quad (31)$$

where $\overleftrightarrow{U}$ and $\overleftrightarrow{V}$ are unitary matrices, $\overleftrightarrow{U} \cdot \overleftrightarrow{U}^\dagger = \overleftrightarrow{1}$. The three real coefficients $\Lambda_u \geq \Lambda_m \geq \Lambda_s \geq 0$ are the singular values of the Singular Value Decomposition (SVD). The Jacobian matrix can also be written as

$$\frac{\partial \vec{x}}{\partial \vec{x}_0} = \hat{U}\Lambda_u\hat{u} + \hat{M}\Lambda_m\hat{m} + \hat{S}\Lambda_s\hat{s}, \quad (32)$$

where $\hat{U}$, $\hat{M}$, and $\hat{S}$ are orthogonal unit vectors, $\hat{U} = \hat{M} \times \hat{S}$, of the unitary matrix $\overleftrightarrow{U}$, which means they define directions in the ordinary space of Cartesian coordinates, $\vec{x}$. The unit vectors $\hat{u}$, $\hat{m}$, and $\hat{s}$ are determined by the unitary matrix $\overleftrightarrow{V}$, which means that they define directions in the space of Lagrangian coordinates, $\vec{x}_0$.

The Jacobian of Lagrangian coordinates, which is the determinant of the Jacobian matrix, is

$$\mathcal{J}_L = \Lambda_u\Lambda_m\Lambda_s. \quad (33)$$

The time derivative $\left(\partial \ln(J_L)/\partial t\right)_L = \vec{\nabla} \cdot \vec{u}_\perp$. For the model of Figure 1 a, the Jacobian changes little from unity.

The properties of evolving magnetic fields and currents using Lagrangian coordinates were discussed by Tang and Boozer [28] in 2000 and by Thiffeault and Boozer [29] in 2003.

3. *Implications of the Cauchy $\vec{B}(\vec{x}, t)$*

Using the Singular Value Decomposition of Lagrangian coordinates, Equation (27) for the Cauchy solution implies [6]

$$B^2 = \left(\frac{\hat{u}^\dagger \cdot \vec{B}_0}{\Lambda_m\Lambda_s}\right)^2 + \left(\frac{\hat{m}^\dagger \cdot \vec{B}_0}{\Lambda_u\Lambda_s}\right)^2 + \left(\frac{\hat{s}^\dagger \cdot \vec{B}_0}{\Lambda_u\Lambda_m}\right)^2. \quad (34)$$

The mathematical definition of a chaotic $\vec{u}_\perp$ is that the largest singular value $\Lambda_u > \exp(t/\tau_L)$ for some $\tau_L > 0$ for any time t greater than a sufficiently large value. The smallest τ_L that satisfies this inequality gives the exponentiation timescale. The product of the three singular values $\Lambda_u\Lambda_m\Lambda_s \approx 1$. When Λ_u increases exponentially, Λ_s decreases exponentially, and Λ_m has at most an algebraic dependence on time. The exponentiation time scale τ_L is usually comparable to the evolution time scale.

The term in B^2 proportional to $(\hat{u}^\dagger \cdot \vec{B}_0)^2$ goes to infinity exponentially in time. The term proportional to $(\hat{s}^\dagger \cdot \vec{B}_0)^2$ goes to zero exponentially. A bounded magnetic field strength is only possible for a time long compared to τ_L when the magnetic field points in the $\hat{M}$ direction,

$$\vec{B}(\vec{x}, t) \to \frac{\hat{m}^\dagger \cdot \vec{B}_0}{\Lambda_u\Lambda_s}\hat{M}. \quad (35)$$

The unit vector $\hat{M}$ is also the unit vector along the magnetic field $\hat{b}$. When the magnetic field is in the $\hat{M}$ direction the current density $\vec{j}$ lies in ribbons along the magnetic field lines which become exponentially wider and exponentially thinner in time with the magnitude of the current density increasing only algebraically [6]. The results of Boozer and Elder [7] in 2021 exhibit these properties.

Any smooth flow must naturally be consistent with the magnetic field lying in the $\hat{M}$ direction. Otherwise the magnetic field pressure $B^2/2\mu_0$ would increase exponentially in time.

The number of spatial dimensions is critical in reconnection theory because the number of singular values of Jacobian matrix equals the number of coordinates. In two dimensions, a chaotic $\vec{u}_\perp$ implies the magnetic field strength must increase exponentially in time, but not in three dimensions.

When $\vec{B}$ has a small component in the $\hat{U}$ direction, that component and the associated current density are amplified exponentially in time until that component becomes comparable to $\vec{B}$. The implication is that localized flows, which are seen in the Huang and Bhattacharjee simulations [5], can produce thin current sheets on a fast time scale as discussed in Section VI A 3.

Although force-limits push $\vec{B}$ to be in the direction $\hat{M}$, which allows only an algebraic increase in current density with time, the small deviations in $\vec{B}$ that are associated with different current profiles can be in the exponentiating $\hat{U}$ direction, which has an exponentially increasing current density. This exponentiation can only hold while the current channel narrows while the spatially-averaged current density remains essentially constant.

IV. EVOLUTION EQUATIONS FOR MAGNETIC FIELD CONNECTIONS, ENERGY, AND HELICITY

A. Conservation of magnetic field line topology

Both the conservation and the evolution of magnetic topology is rigorously defined by the magnetic field line Hamiltonian and its canonical coordinates. Applying a method, which is well known in toroidal plasmas [30], to the model of Figure 1 a, the magnetic field is written using (ψ, θ, z) as coordinates, which map $\vec{x}(\psi, \theta, z, t)$ to ordinary Cartesian coordinates as

$$\vec{x} = x(\psi, \theta, z, t)\hat{x} + y(\psi, \theta, z, t)\hat{x} + z\hat{z}; \tag{36}$$

$$\vec{B} = \frac{\vec{\nabla}\psi \times \vec{\nabla}\theta}{2\pi} + \frac{\hat{z} \times \vec{\nabla}\psi_p}{L}. \tag{37}$$

where ψ is the longitudinal magnetic flux and $\psi_p((\psi, \theta, z, t)$ is the poloidal flux and the field line Hamiltonian,

$$\frac{d\psi}{\partial z} = -\frac{1}{L}\frac{\partial \psi_p}{\partial \theta} \quad \text{and} \quad \frac{d\theta}{\partial z} = \frac{1}{L}\frac{\partial \psi_p}{\partial \psi}. \tag{38}$$

The poloidal flux can be assumed to initially be zero, but it evolves according to the equation

$$\vec{E} + \vec{u} \times \vec{B} = \frac{\partial \psi_p(\psi, \theta, z, t)}{\partial t}\frac{\hat{z}}{L} - \vec{\nabla}\Phi, \quad \text{where} \tag{39}$$

$$\vec{u} = \frac{\partial \vec{x}(\psi, \theta, z, t)}{\partial t} \quad \text{with} \tag{40}$$

$$\vec{E} + \vec{u} \times \vec{B} = -\vec{\nabla}\Phi + \mathcal{E}(\psi, \theta, t)\hat{z}, \quad \text{so} \tag{41}$$

$$\frac{\partial \psi_p}{\partial t} = L\mathcal{E}. \tag{42}$$

Hamilton's equations for the magnetic field lines, Equation (38) change when and only when $\psi_p(\psi, \theta, z, t)$ changes. Consequently, the evolution of ψ_p gives the topological evolution.

The equation $\vec{x}(\psi, \theta, z, t)$ maps the canonical coordinates of the magnetic field line Hamiltonian into Cartesian coordinates. When $\partial\psi_p/\partial t = 0$, the velocity $\vec{u} \equiv \partial\vec{x}/\partial t$ gives the velocity of the magnetic field lines through space.

B. Energy evolution

Power is removed from the magnetic field at the rate $\vec{j} \cdot \vec{E}$. When $\vec{E}$ is given by the Ohm's law of Equation (29), then ignoring the Hall term

$$\vec{j} \cdot \vec{E} = \vec{v} \cdot (\vec{j} \times \vec{B}) + \eta j^2. \tag{43}$$

The term $\vec{v} \cdot (\vec{j} \times \vec{B})$ gives the transfer of energy to plasma, which is not in itself dissipative but can be dissipated by viscosity, Equation (26). The term ηj^2 is the direct Ohmic dissipation of the magnetic energy.

The power that it takes to maintain the divergence-free flow in the top surface,

$$\vec{v}_t = \hat{z} \times \vec{\nabla} h \tag{44}$$

is the integral over the volume of the top surface,

$$\begin{aligned}
\mathcal{P} &= -\int \vec{v}_t \cdot (\vec{j} \times \vec{B}) d^3x && (45)\\
&= \int B_z \vec{j} \cdot \vec{\nabla} h d^3x && (46)\\
&= B_0 \oint h\vec{j} \cdot d\vec{a} = -\frac{B_0}{\mu_0}\int h(\vec{\nabla} \times \vec{B}) \cdot \hat{z} da_t \\
&= -\frac{B_0}{\mu_0}\int \vec{\nabla} \times (h\hat{z}) \cdot \vec{B} da_t \\
&= \frac{B_0}{\mu_0}\int \vec{v}_t \cdot \vec{B}_t da_t, && (47)
\end{aligned}$$

since $\vec{v}_t \cdot \vec{B} = \vec{v}_t \cdot \vec{B}_t$ with $\vec{B}_t$ the tangental magnetic field to the top surface.

The important equations for the power input are Equation (46), which gives the power using the stream function h and the plasma current intercepting the top surface in Figure 1, and Equation (47), which gives the power using the velocity $\vec{v}_t$ of the top surface and the magnetic field tangent to that surface on the plasma side.

C. Helicity evolution

The equation for magnetic helicity evolution was derived in Section VI of Reference [7] and is only summarized here. Letting $g(\vec{x},t)$ be the gauge of the vector potential,

$$\mathcal{K} \equiv \int \vec{A}\cdot\vec{B}d^3x \tag{48}$$

$$= \oint g\vec{B}\cdot d\vec{a} - \frac{2\int \psi_p d\psi d\theta dz}{2\pi L} \tag{49}$$

$$\frac{d\mathcal{K}}{dt} = \dot{K}_B - 2\int \mathcal{E}\frac{d\psi d\theta dz}{2\pi}, \quad \text{where} \tag{50}$$

$$\dot{K}_B = -2B_0^2\int h da_t \quad \text{so} \tag{51}$$

$$\frac{d\mathcal{K}}{dt} = -2B_0^2\int h da_t - 2\int \mathcal{E}\hat{z}\cdot\vec{B}d^3x \tag{52}$$

since the Jacobian of (ψ,θ,z) coordinates is $\mathcal{J} = 1/\hat{z}\cdot(\vec{\nabla}\psi\times\vec{\nabla}\theta) = 1/(2\pi\hat{z}\cdot\vec{B})$.

There are two important points. (1) Helicity is dissipated by the volume integral of $\mathcal{E}B_z$, so neither magnetic field line chaos nor the current density being concentrated into thin ribbons enhances its dissipation. (2) Helicity input occurs when $\int h da_t = \int h r_c dr_c d\theta_c$ is non-zero, where (r_c,θ_c,z) are cylindrical coordinates. The implication is that only the θ_c average of the stream function h contributes, which gives a purely circular flow pattern, $\bar{v}_{\theta_c}(r_c,t)\hat{\theta}_c$. A circular flow can drive ideal kink instabilities, Section IV of Reference [7], and cause the eruption of coronal loops. There is no alternative to an eruption when helicity is systematically accumulating in a loop.

V. RUNAWAY ELECTRONS AND THE CORONA

The large current density j_{shb} that is required to Ohmically dissipate the power input can exceed the Dreicer current density j_d. When $j > j_d$, small-angle Coulomb collisions cannot maintain a near Maxwellian distribution, and electrons runaway to a high energy. The calculations of Kulsrud et al [31] imply the rate of electron runaway reaches a significant value at the current density $j_d = 2\times10^{-2}env_e$.

As pointed out by Boozer in [32] and discussed in [30, 33], when the Dreicer current is exceeded, electrons must runaway to whatever energy is required to carry the current. For the corona, this means to a sufficiently high energy that the electron density n does not become too small due to the gravitational acceleration of the sun g. When the temperature T is constant, $dn/dr = -n/h$, where the scale height $h \equiv T/Mg$. When the ionization is high, $M = m_i$, the proton mass, and $h \approx 350T$ km/eV. A coronal temperature of 100 eV is consistent with a scale height of 35,000 km.

Below the transition region to the corona, Song [34] found the electron temperature is almost constant, ≈ 0.5 eV, which implies an electron thermal speed $v_e \approx 3\times10^5$ m/s and the Spitzer resistivity $\eta \approx 4\times10^{-3}$ Ohm-meter. The electron density drops rapidly with altitude above the photosphere and reaches $n \approx 3\times10^{16}/\mathrm{m}^3$, at the transition. The Dreicer current at the transition is then $j_d \approx 10^5$ A/m^2. The current density $j_{shb} \equiv vB/\eta \approx 250vB$, which equals j_d when $vB \approx 400$ T·m/s. Song found the magnetic field is highly localized in flux tubes on the photosphere, but those tubes have large diameters at the transition region.

The magnetic field and velocity that should be used to estimate of j_{shb} are uncertain and would be better estimated by someone more familiar with solar physics. For coronal loops driven by sunspots, two papers are of particular importance. Okamoto and Sakurai [35] have observed fields above 0.6 T at sunspots, and Sobotka and Puschmann [36] have observed horizontal flows of 4 km/s. The product of these numbers gives $vB = 2400$ T·m/s approximately six times higher than that required for $j_d = j_{shb}$ at the transition. More typical velocities and fields could produce an exact balance.

As noted in [30], any star that has evolving magnetic field structures on the scale of tens of thousands of kilometers must have a corona, otherwise the induced currents would run out of current carriers, but whether this actually explains the solar corona requires careful study.

VI. SIMULATIONS BY HUANG AND BHATTACHARJEE

The Huang and Bhattacharjee [5] publication *Do chaotic field lines cause fast reconnection in coronal loops?* is of sufficient importance to be a Featured article by the Physics of Fluids and is the most complete numerical study of the importance of chaos to

reconnection in the solar corona. They carried out the simulations in a model equivalent to Figure 1 a, recognized that magnetic fields that depend on all three spatial coordinates are generically chaotic and noted that: *Boozer points out the fragility of the ideal MHD frozen-in constraint in the presence of chaotic field lines. This important aspect warrants a broader attention and further investigation.*

Nevertheless, the Huang-Bhattacharjee paper is skeptical about the importance of chaos to reconnection. They dismiss the importance of changes in field-line connections that arise from the exponential enhancement of resistive diffusion by chaos: *Boozer's definition of reconnection relies entirely on the connections between fluid elements, and he attributes any changes in the connections to reconnection. This definition, while precise, is overly general, and blurs the distinction between reconnection and diffusion.* What they view as important are the *signatures of reconnection*, intense current densities $j \approx j_{shb}$, which are required to dissipate the input power. The skepticism of Huang and Bhattacharjee comes from different views about what are the important questions in reconnection theory and what are the important features of a model. These differences were discussed in Section II.

Even in their abstract [5], Huang and Bhattacharjee focus criticism on a paper by Boozer and Elder [7]. The Boozer-Elder paper used the model of Figure 1 a for an in-principle proof that boundary conditions that force the magnetic field lines to be chaotic can make a change in the connections of magnetic field lines inevitable on a fast timescale. This timescale is set by the boundary conditions regardless of how small the non-ideal plasma effects may be.

As discussed in Boozer's 2021 paper [6], as field-line connection changes proceed, static force balance is lost and the evolution rate is *determined by the speed of Alfvén waves.* Since the plasma current density required for consistency with the chaos is smaller by a factor $\ln(R_m)/R_m$ than that required for dissipating the input power, the input power must cause plasma velocity $\tilde{v}$ and magnetic field $\tilde{B}$ perturbations of increasing amplitude until dissipation balances the input power.

As expected, rapid plasma flows are seen in the Huang-Bhattacharjee simulations after changes in field line connections become inevitable, Section VI A 2, but they claim disagreement with the equation used by Boozer and Elder, $\partial K(\ell,t)/\partial t = \partial\Omega(\ell,t)/\partial\ell$, for the parallel current density. This simplified equation assumes currents distant from the magnetic field line being considered make a negligible contribution to $\nu(\ell,t)$, the rotational transform per unit length, of Equation (5). The validity of this approximation requires no kinks arise, and Boozer and Elder chose a chaotic flow $\vec{v}_t$ that has a special form that does not drive kink instabilities. Indeed, Huang and Bhattacharjee saw no evidence of instabilities during their ideal, $\eta = 0$ simulations.

With the approximation $\partial K/\partial t = \partial\Omega/\partial\ell$, Boozer and Elder showed that before changes in field line connections take place that a simplified version is adequate with $\partial\Omega/\partial\ell = \Omega_t/L$, where Ω_t is the vorticity in the top surface. The resulting model is extremely simple but shows how the current density naturally concentrates in exponentially thin but broad ribbons with the maximum current density only increasing linearly in time.

The Boozer and Elder approximation can only be valid up to the point at which magnetic reconnection is inevitable. Afterwards, rapid flows make $\partial\Omega/\partial\ell >> \Omega_t/L$. Section VI A 3 shows the equation $\partial K/\partial t = \partial\Omega/\partial\ell$ gives the time required for the current density to reach the large values seen in the Huang-Bhattacharjee simulations that is extremely short, $\sim a/V_A$, when parameters are used that are characteristic of the period after fast reconnection has begun.

The primary criticism that Huang and Bhattacharjee make of the Boozer-Elder calculation is the omission of the term $\mathcal{T}$, Equation (6). As discussed in Section III A 2, this term appears to be analogous to $\partial\nu/\partial t$ of Equation (5), and would apparently add a term to K that equals $-k_z(\Delta_q^2 + \Delta_s\Delta_q/2)(2a^2)$, where k_z is the wavenumber of the variation of the field-line displacements, the Δ's, along the line. This term can be significant before strong field line breaking occurs. Nevertheless, as the Boozer-Elder calculation proves, it is not necessary for the breaking of connections to become inevitable on a fast time scale, which was the motivation for their calculation. Ignoring this term, they found exponentially increasing distortions of the tubes of magnetic field lines and exponentially thinning and broadening ribbons of current.

Since numerical errors are multiplied by an exponential, it is difficult to accurately follow a force-free ideal evolution, which requires the field $\vec{B}(\vec{x},t)$ preserve the footpoint locations while $(\vec{\nabla}\times\vec{B})_\perp = 0$, as the number of exponentiations in separation between neighboring pairs of field lines becomes arbitrarily large.

A. Interpretation of the simulations

Basic physics gives an interpretation of the Huang and Bhattacharjee simulations. The estimates made in this section could obviously be made far more accurately by the simulation authors.

1. Dimensional analysis

Simple scalings can be made by dimensional analysis of the fundamental equations. Equation (46) implies the input power $P_{in} \approx B_0 v_t a \bar{j} A_t$, where $A_t = a^2$ is the area of the top surface, the stream function $h \approx a v_t$, and $\bar{j}$ is a spatially averaged current density. The resistively dissipated power $P_\eta = \eta j_c^2 f_A A_t L$, where f_A is the fraction of the area occupied by the concentrated current density j_c, so $j_c = \bar{j}/f_a$. For a balance, $P_\eta = P_{in}$,

$$j_c \approx \frac{v_t B_0}{\eta}\frac{a}{L} \tag{53}$$

$$= R_m \frac{B_0}{\mu_0 L}, \text{ and} \tag{54}$$

$$\frac{B_0}{\mu_0 L} = \frac{\delta B}{\mu_0 a} = \bar{j}, \text{ so} \tag{55}$$

$$j_c \approx R_m \bar{j} \text{ and} \tag{56}$$

$$f_A \approx \frac{1}{R_m}. \tag{57}$$

The perturbed magnetic field consists of two parts. A part $\delta B \approx B_0 a/L$ is required for field lines to connect appropriately at the top and bottom surfaces of the cylinder. Another part is a fluctuating field $\tilde{B} \approx (\tilde{v}/V_A)B_0$ due to Alfvén waves talking up the released energy. The energy in Alfvén waves must increase until the vorticity $\Omega = \hat{b}\cdot\vec{\nabla}\times\vec{\tilde{v}}$ becomes sufficiently strong to increase the concentrated current to the level required for power balance.

2. Scaling coefficients

More precise scalings can be obtained by modifying the dimensional analysis by multiplicative coefficients to obtain agreement with Line E in Table I of their paper. All the coefficients are small. It would be interesting to study why.

The non-fluctuating part of the perturbed part of the magnetic field δB needs to be of order $(a/L)B_0 = 0.1B_0$ to connect the footpoints at the top and bottom of the cylinder. $E_M = \int(\delta B^2/2)d^3x = 4.37\times10^{-3}B_0 a^2 L$ implies

$$\delta B = 0.296 B_0. \tag{58}$$

The oscillatory part of the perturbed magnetic field $\tilde{B} = B_0\tilde{v}/V_A$ also has the magnitude $\tilde{B} \approx 0.1B_0$ but only in the small fraction of the cross-sectional area

$$f_A = 1.63\times10^{-3} \tag{59}$$

in which the current is concentrated. The factor $\tilde{v}/V_A$ in the narrow regions of current concentration can be obtained from their Figure 6, as $\tilde{v} \approx 0.1V_A$ and from the kinetic energy $E_K = 8.97\times10^{-6}$ divided by the fraction of the cross-sectional area occupied by these currents, f_A, so $\tilde{v}^2/2V_A^2 = 5.5\times10^{-3}$, which gives

$$\frac{\tilde{v}}{V_A} = 0.105. \tag{60}$$

The power input over a run of length $10^3 a/V_a$ is

$$W_p = (B_0/\mu_0)\int \vec{B}_\perp\cdot\vec{v}_t dadt \tag{61}$$

$$= c_p 0.296 B_0 \times 10^{-2} V_a \times a^2 \times 10^3 a/V_A \tag{62}$$

$$= 2.96 c_p (B_0^2/\mu_0) a^3 \tag{63}$$

$$= 1.79\times10^{-2}(B_0^2/\mu_0)a^3, \text{ from Table I;} \tag{64}$$

$$c_p = 6.05\times10^{-3}. \tag{65}$$

using the entry for the $S = 10^6$ case from Table I.

The density of the concentrated current is

$$j_c = c_j \frac{\delta B}{\mu_0 a f_A} \tag{66}$$

$$= 181.6 c_j \frac{B_0}{\mu_0 a} \tag{67}$$

$$= 9.69\frac{B_0}{\mu_0 a} \text{ from Table I;} \tag{68}$$

$$c_j = 5.33\times10^{-2}. \tag{69}$$

The energy dissipated by resistively is

$$W_\eta = \int \eta j^2 d^3x dt \tag{70}$$

$$= c_\eta(\eta j_c^2 f_A a^2 L)\left(10^3\frac{a}{V_A}\right), \text{ so} \tag{71}$$

$$= c_\eta \eta \left(c_j\frac{B_0}{\mu_0 a}\right)^2 (f_A a^2 L)\left(10^3\frac{a}{V_A}\right) \tag{72}$$

$$= c_\eta\eta(0.1B_0)(f_A a\mu_0)^2(f_A L)(10^2 a/V_A) \tag{73}$$

$$= \frac{c_\eta c_j^2 f_A}{S}\frac{L}{a}\frac{B_0^2}{\mu_0}a^3 \tag{74}$$

$$= 0.463 c_\eta \frac{B_0^2}{\mu_0}a^3 \tag{75}$$

$$= 1.13\times10^{-2}\frac{B_0^2}{\mu_0}a^3 \text{ from Table I;} \tag{76}$$

$$c_\eta = 24.4\times10^{-3}, \tag{77}$$

which is approximately four times larger than c_p.

3. Time required to reach j_c

The time required to reach a current density j_c is given by $\partial K/\partial t = \partial\Omega/\partial\ell$, where $K \equiv \mu_0 j_c/B_0$.

When viscous effects are small, kinetic terms must balance the $\vec{j} \times \vec{B}$ force. Once the velocity fluctuations are large, it is natural to expect $|\partial\vec{v}/\partial t| \approx |\vec{v} \cdot \vec{\nabla}\vec{v}| \approx \tilde{v}^2/\delta_{tan}$ where δ_{tan} is the scale of $\vec{v}$ variation along itself. Figure 6 of Huang and Bhattacharjee's paper [5] implies the spatial scale over which $\tilde{v}$ changes along itself is much greater than the distance it changes across the flow direction, $\delta_\perp$. This disparity in scales is related to the concentrated current lying in thin but broad ribbons along the magnetic field lines as seen by Boozer and Elder and predicted in [6]. The implication is that $|\partial\vec{v}/\partial t| \approx (V_A/\delta_\ell)\tilde{v} \approx \tilde{v}^2/\delta_{tan}$, so $\delta_\ell \approx (V_A/\tilde{v})\delta_{tan}$.

The rate at which the current increases in the regions of concentrated current is $\partial K_c/\partial t \approx (\tilde{v}^2/V_A)/(a^2 f_A)$, where $K_c \equiv \mu_0 j_c/B_0$ and $f_A = \delta_{tan}\delta_\perp/a^2$. Consequently, the time require for K to reach K_c

$$t_c \approx c_j \frac{\delta B}{B_0}\left(\frac{V_A}{\tilde{v}}\right)^2 \frac{a}{V_A} \quad (78)$$

$$\approx 1.43\frac{a}{V_A}. \quad (79)$$

The time to reach j_c can also be estimated by how long it takes to put the required energy into Alfvén waves, which is $2E_K = 1.794 \times 10^{-5}$ in the units of the Huang-Bhattacharjee paper. The required time to drive the Alfvén waves is

$$t_a \equiv \frac{2E_K\left(10^3 \frac{a}{V_A}\right)}{W_p} \quad (80)$$

$$\approx 1.0\frac{a}{V_A}, \quad (81)$$

which is consistent.

The energy in the large scale field δB is little changed by whether that field is produced by highly localized or by a smooth current density.

B. Importance of viscosity

Dissipation can balance the input power in two ways: resistive dissipation ηj^2 and viscous dissipation $\rho\nu\vec{\Omega}^2$, where $\vec{\Omega} \equiv \vec{\nabla} \times \vec{v}$, integrated over the plasma volume. The strength of the inertial relative to the viscous force is measured by the ordinary fluid Reynolds number $R_f \equiv va/\nu$. The ratio $R_m/R_f = \mu_0\nu/\eta \equiv P_r$ is the plasma Prandtl number, which is generally much larger than unity in plasmas [37].

The Huang and Bhattacharjee simulations [5] studied the effect of the Prandtl number on dissipation with simulations at $R_m \approx 10^4$, which is equivalent to $S = 10^6$, at fluid Reynolds numbers of $R_f \approx 10^4$ and $R_f \approx 10$. They found the fraction of the power dissipated by viscosity increased from 16% to 33% as the fluid Reynolds number was decreased. Since resistivity was the dominate source of dissipation, the maximum current density remained $j \approx j_{shb}$. The scaling of the fraction of the dissipation due to resistivity for R_f below unity was not explored. The equation for the plasma flow velocity greatly simplifies when R_f is much less than unity, $\rho\nu\vec{\nabla} \times \vec{\Omega} = -\vec{j} \times \vec{B}$ with $\Omega \equiv \vec{\nabla} \times \vec{v}$. Although this limit could have been explored, it was not.

For the viscosity to compete, need $\nu\tilde{v}/\delta_\perp^2 \approx \tilde{v}^2/\delta_{\rm tan}$, or $\nu \approx \tilde{v}(\delta_\perp^2/\delta_{tan}) \approx \tilde{v}(\delta_\perp^3/A_t f_A) \approx R_m(\delta_\perp^2/a^2)\delta_\perp\tilde{v}$. Figure 6 of Huang and Bhattacharjee implies the perturbed plasma velocity during fast reconnection reaches $\tilde{v} \approx 0.1V_A$ and the width of the high velocity region $\delta_\perp \approx 10^{-2}a$. Consequently, $\nu \approx 10^4 \times 10^{-4} \times 10^{-2} \times 10^{-1} = 10^{-3}$, and $R_f = av_t/\nu \approx 10$ is required for viscosity to compete with inertia. The actual fluid Reynolds number when the Prandtl number $P_r = 10^3$ and the magnetic Reynold number is 10^4 is $R_f = 10$, which is equivalent to Run H in the Huang and Bhattacharjee Table II. It would appear that their simulations did not consider a case in which viscosity is dominant over inertial effects.

VII. DISCUSSION

The evolution of magnetic fields in low-resistivity plasmas has three parts: the evolution of the topology of the magnetic field lines, the evolution of the magnetic energy, and the evolution of the magnetic helicity. Two effects can greatly modify the rates of evolution, the concentration of the current density into thin but broad ribbons along the magnetic field lines and chaos in the magnetic field line trajectories. Chaos, or more precisely deterministic chaos, means neighboring pairs of field lines separate exponentially with distance along the lines within a bounded region of space. Only magnetic field lines that have an exponential dependence on all three spatial dimensions can be chaotic; Reference [38] discusses the history and importance of the concept of chaos.

The three parts of the evolution respond in fundamentally different ways to the concentration of the current density and to chaos when the resistivity is small. A magnetic Reynolds number $R_m \equiv \mu_0 va/\eta \gtrsim 10^4$ is typical of laboratory plasmas, and $R_m \sim 10^{14}$ is not unusual in solar and astrophysical plasmas.

Magnetic field lines cannot change their topology when $\hat{b} \cdot \vec{E} = -\partial\Phi/\partial\ell$ with $\hat{b} = \vec{B}/B$ and ℓ is the

distance along a field line, for then $\partial\vec{B}/\partial t = \vec{\nabla}\times(\vec{u}\times\vec{B})$ and $\vec{u}$ is the velocity of the field lines, [26]. Away from nulls in the magnetic field, a potential $\Phi(\vec{x},t)$ can always be found that locally satisfies $\hat{b}\cdot\vec{E} = -\partial\Phi/\partial\ell$. But, such a $\Phi(\vec{x},t)$ does not exist in a torus when along a given line

$$\lim_{L\to\infty}\frac{1}{L}\int_0^L \hat{b}\cdot\vec{E}d\ell \neq 0, \tag{82}$$

nor when $\hat{b}\cdot\vec{E}$ integrated from one perfectly-conducting boundary to another is non-zero. When a Φ does not exist that globally satisfies $\hat{b}\cdot\vec{E} = -\partial\Phi/\partial\ell$, the introduction of a term $\mathcal{E}\vec{\nabla}\ell$ with $\hat{b}\cdot\vec{\nabla}\mathcal{E} = 0$, as in Equation 28 solves the non-locality issue.

When magnetic field lines leave the volume in which calculations are made, adequate boundary conditions for determining whether magnetic field lines break or not are extremely subtle [21]. Topology changes in magnetic field lines are well defined only when $\mathcal{E}$ is.

The importance of chaos to the preservation of magnetic field line connections is undeniable when Faraday's law and mathematics are accepted. When magnetic field lines are evolving in a way that increases the rate at which they exponentiate apart, a non-zero $\mathcal{E}$ will cause a breaking of connections on a timescale that depends only logarithmically on the magnitude of $\mathcal{E}$.

The breaking of magnetic field line connections removes a constraint on magnetic evolution, but its connection with the transfer of energy from the magnetic field to the plasma is complicated. When the magnetic field evolution is ideal, the power transfer to the plasma is $\int \vec{u}_\perp\cdot(\vec{j}\times\vec{B})d^3x$. The $\vec{j}\times\vec{B}$ Lorentz force integrated over a thin current layer need not be large. A delta-function current density is equivalent to a current potential κ, which produces only a finite force on the current carrier [39]. A large power transfer occurs only when the flow velocity $\vec{u}$ is also concentrated in the thin layer.

When power is continuously put into the plasma, there are two ways it can be dissipated: by resistively $\int \eta j^2 d^3x$ and by viscosity $\int \rho\nu(\vec{\nabla}\times\vec{v})^2 d^3x$. An important but unsettled question is what fraction of the power is dissipated by viscosity versus resistivity in the limit as the magnetic Reynolds number $R_m \to \infty$. When the viscosity is extremely large, it would seem difficult to for the flow velocity to lie in thin layers, which seems necessary to form the thin layers of intense j that are necessary for a large resistive dissipation. Is this true only when the fluid Reynolds number $R_f = av/\nu$ is less than unity? Or, can it be true when the Prandtl number $P_r = R_m/R_f = \mu_0\nu/\eta$ becomes sufficiently large even with $R_f >> 1$? Practical simulations can certainly determine the nature of reconnection for R_f arbitrarily small, but practical limitations on the highest R_m that can be simulated may prevent studies of the case with a very large Prandtl number but with $R_f > 1$.

Magnetic field line chaos and intense current sheets have little effect on the evolution of magnetic helicity. It is important to study what happens when footpoint motion injects helicity into a solar loop. Presumably, the loop becomes kink unstable and must eventually erupt from the sun. This could be studied in the model of Figure 1.a with the region directly driven by the footpoint motion of much smaller radius that the radius of the cylinder as described in [7].

Electron runaway offers a compelling explanation of the solar corona and serves as a check on the production of intense currents by even smooth, large-scale footpoint motion. The more complete measurements and more powerful simulations should allow a far better understanding.

Acknowledgements

This work was supported by the U.S. Department of Energy, Office of Science, Office of Fusion Energy Sciences under Award Numbers DE-FG02-95ER54333, DE-FG02-03ER54696, DE-SC0018424, and DE-SC0019479.

Data availability statement

Data sharing is not applicable to this article as no new data were created or analyzed in this study.

[1] E. N. Parker and M. Krook, *Diffusion and severing of magnetic lines of force*, Ap. J. **124**, 214 (1956): doi10.1086/146216.

[2] M. Hesse and P. A. Cassak, *Magnetic Reconnection in the Space Sciences: Past, Present, and Future*, Journal of Geophysical Research: Space Physics **125**, e2018JA025935 (2020): doi.org/10.1029/2018JA025935.

[3] K. Schindler, M. Hesse, and J. Birn, *General magnetic reconnection, parallel electric-*

fields, and helicity, Journal of Geophysical Research—Space Physics **93**, 5547 (1988): doi10.1029/JA093iA06p05547.

[4] Karl Popper, *The Logic of Scientific Discovery*, (Hutchinson & Co, 1959) and *Logik der Forschung*, (Julius Springer,1934).

[5] Y.-M. Huang and A. Bhattacharjee, *Do chaotic field lines cause fast reconnection in coronal loops?*, Phys. Plasmas **29**, 122902 (2022): doi10.1063/5.0120512.

[6] A. H. Boozer, *Magnetic reconnection and thermal equilibration*, Phys. Plasmas **28**, 032102 (2021): doi10.1063/5.0031413.

[7] A. H. Boozer and T. Elder, *Example of exponentially enhanced magnetic reconnection driven by a spatially bounded and laminar ideal flow*, Phys. Plasmas **28**, 062303 (2021): doi10.1063/5.0039776.

[8] D. Borgogno, D. Grasso, F. Porcelli, F. Califano, F. Pegoraro, and D. Farina, *Aspects of three-dimensional magnetic reconnection*, Phys. Plasmas **12**, 032309 (2005): doi10.1063/1.1857912.

[9] A. Lazarian, G. L. Eyink, A. Jafari, G. Kowal, H. Li, S-Y Xu, and E. T. Vishniac, *3D turbulent reconnection: Theory, tests, and astrophysical implications*, Phys. Plasmas **27**, 012305 (2020): doi10.1063/1.5110603

[10] E. Priest, *MHD structures in three-dimensional reconnection*, *Book Series Astrophysics and Space Science Library*, *Magnetic reconnection: concepts and applications*, volume **427**, page 101 (Springer International Publishing 2016, edited by WalterGonzalez and Eugene Parker): doi10.1007/978-3-319-26432-5-3.

[11] J. Reid, C. E. Parnell, A. W. Hood, and P. K. Browning, *Determining whether the squashing factor, Q, would be a good indicator of reconnection in a resistive MHD experiment devoid of null points*, Astronomy and Astrophysics **633**, A92 (2020): doi10.1051/0004-6361/201936832.

[12] A. H. Boozer, *Runaway electrons and ITER*, Nucl. Fusion **57**, 056018 (2017): doi10.1088/1741-4326/aa6355.

[13] A. H. Boozer, *The rapid destruction of toroidal magnetic surfaces*, Phys. Plasmas **29**, 022301 (2022): doi10.1063/5.0076363.

[14] S. C. Jardin, N. M. Ferraro, W. Guttenfelder, S. M. Kaye, and S. Munaretto, *Ideal MHD Limited Electron Temperature in Spherical Tokamaks*, Phys. Rev. Lett. **128**, 245001 (2022): doi10.1103/PhysRevLett.128.245001.

[15] M. A. Berger, *Rigorous new limits on magnetic helicity dissipation in the solar corona*, Geophysical and Astrophysical Fluid Dynamics, **30**, 79 (1984): doi10.1080/03091928408210078.

[16] A. H. Boozer, *Ohm's Law for mean magnetic fields*, J. Plasma Physics **35**, 133-139 (1986): doi10.1017/S0022377800011181.

[17] A. Bhattacharjee and Y. Yuan, *Self-consistency constraints on the dynamo mechanism*, Ap. J. **449**, 739 (1995): doi10.1086/17609.

[18] F. Rincon, *Dynamo theories*, J. Plasma Phys. **85**, 205850401 (2019): doi10.1017/S0022377819000539.

[19] T. S. Kuhn, *The Structure of Scientific Revolutions* (University of Chicago Press, Chicago and London, 1962): ISBN 9780226458113.

[20] Britannica, The Editors of Encyclopaedia (2021, July 14). "Thomas S. Kuhn." Encyclopedia Britannica. https://www.britannica.com/biography/Thomas-S-Kuhn.

[21] A H. Boozer, *Magnetic reconnection in space*, Phys. Plasmas **19**, 092902 (2012):doi10.1063/1.4754715.

[22] A. H. Boozer, *Local analysis of fast magnetic reconnection*, Phys. Plasmas **29**, 052104 (2022): doi10.1063/5.0089793.

[23] A. H. Boozer, *Erratum: Local analysis of fast magnetic reconnection*, to be published Phys. Plasmas.

[24] D. P. Stern, *The motion of magnetic field lines*, Space Science Reviews **6**, 147 (1966): doi10.1007/BF00222592.

[25] A. H. Boozer, *Plasma equilibrium with rational magnetic surfaces*, Phys. Fluids **24**, 1999 (1981): doi10.1063/1.863297.

[26] W. A. Newcomb, *Motion of magnetic lines of force*, Ann. Phys. **3**, 347 (1958): doi10.1016/0003-4916(58)90024-1.

[27] T. Elder and A. H. Boozer, *Magnetic nulls in interacting dipolar fields*, J. Plasma Phys. **87**, 905870225 (2021): doi10.1017/s0022377821000210.

[28] X. Z. Tang and A. H. Boozer, *Anisotropies in magnetic field evolution and local Lyapunov exponents*, Phys. Plasmas **7**, 1113 (2000): 10.1063/1.873919.

[29] J. L. Thiffeault and A. H. Boozer, *The onset of dissipation in the kinematic dynamo*, Phys. Plasmas **10**, 259 (2003): doi10.1063/1.1528902.

[30] A. H. Boozer, *Physics of magnetically confined plasmas*, Rev. Mod. Phys. **76**, 1071 (2004).

[31] R. M. Kulsrud, Y.-C. Sun, N. K. Winsor, and H. A. Fallon, *Runaway electrons in plasma*, Phys. Rev. Lett. **31** 690 (1973): doi10.1103/PhysRevLett.31.690

[32] A. H. Boozer, *Implications of magnetic Helicity conservation*, "Magnetic helicity in space and laboratory plasmas," edited by M. R. Brown and R. C. Canfield (American Geophysical Union, Washington, DC, 1999) p.11-16.

[33] A. H. Boozer, *Particle acceleration and fast magnetic reconnection*, Phys. Plasmas **26**, 082112 (2019); doi10.1063/1.5094179.

[34] P. Song, *A model of the solar chromosphere: structure and internal circulation*, Ap. J. **846**, 92 (2017): doi10.3847/1538-4357/aa85e1.

[35] T. Okamoto and T. Sakurai *Super-strong magnetic field in sunspots*, Ap. J. Lett. **852**, L16 (2018): doi10.3847/2041-8213/aaa3d8.

[36] M. Sobotka and K. G. Puschmann, *Horizontal motions in sunspot penumbrae*, Astronomy and Astrophysics **662**, A13 (2022): doi10.1051/0004-6361/202243577.

[37] M. J. Aschwanden, *Physics of the solar corona*, (Springer 2006, ISBN 3540307656), Section 7.5.

[38] R. Bishop, *Chaos* in the Stanford Encylopedia of Philosophy, Spring 2017 {editor: E. N. Zalta, Meta-

physics Research Lab, Stanford University}, https://plato.stanford.edu/entries/chaos/.

[39] A. H. Boozer, *The interaction of the ITER first wall with magnetic perturbations*, Nucl. Fusion **61**, 046025 (2021): doi10.1088/1741-4326/abe226.